Nucleation Antibunching in Catalyst-Assisted Nanowire Growth

Frank Glas,* Jean-Christophe Harmand, and Gilles Patriarche

CNRS-Laboratoire de Photonique et de Nanostructures, Route de Nozay, 91460 Marcoussis, France

(Received 8 January 2010; published 31 March 2010)

We elaborate $InP_{1-x}As_x$ nanowires by vapor-liquid-solid growth, with small and short composition oscillations produced on purpose with a constant time period. The lengths of these oscillations, measured in single wires by transmission electron microscopy, give access to instantaneous growth rates and their distribution reveals the nucleation statistics. We find that these statistics are strongly sub-Poissonian, which proves that the nucleation events are anticorrelated in time. This effect, specific to nanovolumes, efficiently regulates nanowire growth. We explain it by the rapid depletion of the catalyst droplet in group V atoms upon forming each monolayer of the nanowire.

DOI: 10.1103/PhysRevLett.104.135501 PACS numbers: 81.07.Gf, 81.05.Ea, 81.15.Kk, 82.60.Nh

Nanosize effects are known to modify the thermodynamics and kinetics of a system. For instance, the large surface/volume ratio of a nanoparticle affects the chemical potentials of its constituents and hence phase diagrams [1,2] and nucleation rates during phase transformations. Surface may also be a privileged locus for nucleation [3,4]. Still, although nucleation of a new phase in a nanoparticle is a problem of deep fundamental and practical import, this elusive effect remains scarcely studied.

Semiconductor nanowires (NWs) formed in the vapor-liquid-solid (VLS) growth mode are a case in point. In VLS growth, atoms transfer from a vapor to the solid NW via a liquid catalyst nanodrop sitting at the top of the NW [5]. Nucleation is of paramount importance here because, given the small size of the condensation area (the droplet-NW interface), growth entails the repeated nucleation of two-dimensional atomic or biatomic layers (monolayers, MLs). The growth rate of the NW [6], its crystal structure [4,7], or the abruptness of the heterointerfaces that it may contain [8] are all governed by nucleation.

Most experimental studies assess the kinetics of NW growth from postgrowth measurements of the final lengths of NWs fabricated at several given growth times [6,9–11]. This is unsatisfactory since such measurements cannot record the transient or nonlinear growth regimes that have been predicted [9,10,12]; moreover, since different sets of NWs are examined for each growth time, unwarranted assumptions have to be made to extract generic behaviors. The insertion in the NW of markers made of thin layers of a different material is more informative [13]. However, fine variations of growth rate cannot be measured in this way and the insertion of the marker itself can alter the growth kinetics. Conversely, *in situ* transmission electron microscopy (TEM) experiments [2,14,15] accurately record the instantaneous growth rate of individual NWs down to the ML [8], but they are currently limited in terms of growth methods and material systems. Here, we propose a simple method that overcomes some of these limitations and allows one to investigate finely the growth of single NWs from a vapor. We show that it yields key information about growth kinetics and nucleation statistics.

Our method applies as soon as the NW contains two elements having a certain miscibility range. It relies on periodic modulations of the incident vapor fluxes produced on purpose. The amplitude and time period τ of the flux modulation are chosen to produce small but detectable oscillations in the composition of the NW along the growth direction (the modulation must be small enough to minimize the ensuing perturbation on NW growth kinetics). Since the period τ is fixed, an *ex situ* measurement of the oscillation lengths yields the instantaneous growth rate at each time period. This gives access to the complete chronology of growth of single NWs.

For III–V or II–VI compounds, a ternary alloy at least is required to obtain a composition modulation. We apply the method to $InP_{1-x}As_x$ NWs grown at 420 °C by Au-catalyzed molecular beam epitaxy on (111)B oriented InP substrates. As_4 and P_2 fluxes are evaporated from solid sources and a periodic modulation of the incident $As_4 : P_2$ flux ratio is produced. Here, the modulation is obtained indirectly, at constant source fluxes, by exploiting the spatial nonuniformity of the beams: the sole substrate rotation suffices to generate small local modulations of the incident fluxes with a very stable time-period equal to the rotation period and an amplitude tunable by selecting NWs grown at different distances from the rotation axis. A time period $\tau = 3.6$ s was chosen, during which 10 to 30 MLs form (1 ML $\simeq$ 0.34 nm). The low solubilities of the group V species in the catalyst [9,16,17] favor the transfer of the vapor flux modulation to the liquid whereas modulations of group III fluxes might get damped since the droplet acts as a reservoir for these highly soluble elements [energy dispersive x-ray spectroscopy (EDXS) yields postgrowth droplet compositions of about $Au_{0.5}In_{0.5}$].

Our NWs have a perfect wurtzite crystal structure and grow in the [0001] direction, each with a uniform diameter set by the size of its catalyst droplet [Fig. 1(a)]. Hence, nucleation at the NW sidewalls is negligible and we probe

the sole axial growth. After growth, the NWs are dispersed on a thin membrane and imaged by high angle annular dark field (HAADF) Cs-corrected scanning TEM (STEM), a technique very sensitive to composition variations [18]. In Fig. 1(a), the faint contrast along the growth axis confirms that the composition of the NW has indeed been modulated. The oscillation amplitude is about $\pm 0.7\%$ of the total HAADF intensity. The corresponding variation of the As concentration x was determined by EDXS to be $\Delta x \simeq \pm 0.03$ around a mean value of 0.66. The positions of the oscillation extrema can be measured over the whole length of a single NW using overlapping HAADF images.

The measurement of the variation with growth time t of the length L of a NW illustrates the potential of the method [Fig. 1(b)]. A nonlinear $L(t)$ dependence has been predicted by several NW growth models [9,10,12]. Our experiments corroborate this behavior, explainable by the efficient transfer to the drop of vapor atoms impinging on the NW sidewalls: a lengthening NW collects more such atoms and thus grows faster. Our data can be well fitted by the models of Dubrovskii *et al.* [12] [Fig. 1(b)] or Plante and LaPierre [10]. From this study (to be detailed elsewhere), we estimate surface diffusion lengths and chemical potentials and deduce that sidewall collection quickly becomes the main contribution to NW growth.

In the following, we focus on one of the major interests of our method, namely, that it permits the nucleation statistics to be investigated. To this end, the length of each composition oscillation must be determined precisely. To increase the HAADF signal to noise ratio, we study rather thick NWs and fast-Fourier-transform and filter the raw images [Fig. 1(a)]. The length of each oscillation is then measured to within ± 1 ML [Fig. 2(a)].

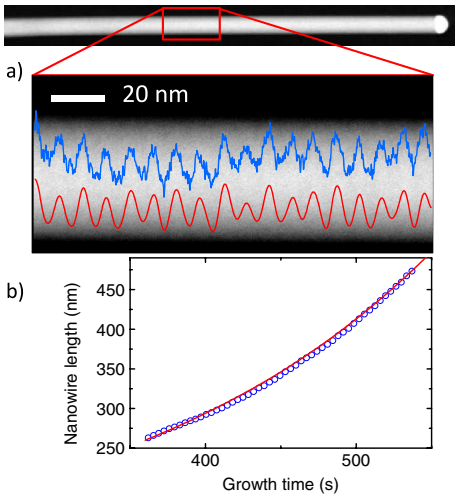

FIG. 1 (color online). $InP_{1-x}As_x$ NW grown with a modulated $As_4 : P_2$ flux ratio. (a) HAADF STEM images reveal composition oscillations. Upper line: HAADF signal integrated across the NW and plotted along the growth axis. Lower line: same profile after Fourier filtering. (b) Length of the NW as a function of total growth time measured from the composition oscillations (circles) and fitted with Dubrovskii's model [12] (line).

It is generally admitted that the formation of NWs of small enough radii requires one and only one nucleation event for growing each new ML. This *mononuclear* regime [19], whereby a ML grows in a time much shorter than the mean time between two successive nucleation events, is indirectly supported for III–V NWs [4,20] and has now been directly observed for group IV NWs [8]. In this regime, the growth rate is fixed by the rate of nucleation at the catalyst-solid interface and the number of MLs grown equals the number of nucleation events. The length of each oscillation (in MLs) thus equals the number of nucleation events in time period τ.

If these nucleation events occurred independently of each other, the probability of a given number m of nucleations taking place during τ should follow Poisson statistics. This is the assumption of classical nucleation theory, which is made implicitly or explicitly [21] to model NW growth from nucleation probabilities. Figure 2(b) compares the distribution of the oscillation lengths with a Poisson distribution normalized to the same total number of oscillations [22]. The nucleation statistics are markedly sub-Poissonian. In the three NW segments studied, the experimental standard deviations σ are less than half the Poisson standard deviations (Table I). This proves that the nucleation events are not independent.

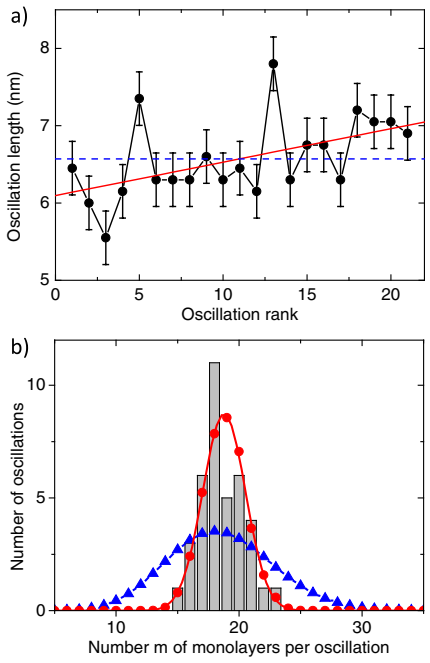

FIG. 2 (color online). Experimental determination of the nucleation statistics. (a) Length of successive oscillations (segment 3 of Table I). The dashed line gives the mean length; the solid line is a linear regression ($dL/dt \propto t$). (b) Histogram of the numbers of nucleation events per oscillation (cumulated from segments 2 and 3; see Table I). The two curves represent distributions calculated for a large number of nucleation events and normalized to the total number of experimental counts: Poissonian statistics (triangles), self-regulated statistics (disks).

The independence of successive nucleation events, which results in Poisson statistics, may be a reasonable assumption for a supersaturated medium of *macroscopic* dimensions, the state of which is only negligibly modified by each nucleation. On the contrary, forming a new ML from a nanodrop consumes a significant fraction of the constituents of the latter [8,23] and suddenly modifies its thermodynamic state. This can explain the peculiar statistics that we observe. Assume that, after each successful nucleation, ML completion occurs in a time negligible as compared with the mean time between nucleations [4,7,8,19]. This causes an abrupt decrease of the numbers of group III and group V atoms in the liquid and hence (since Au is conserved) of their concentration, of their chemical potential, and of the nucleation probability, which do not recover their prenucleation values before the drop is refilled. Conversely, overfilling of the drop due to a temporary lack of nucleation, leads to an increase of the nucleation probability. Nucleation is thus less likely after a nucleation event than before, nucleation events are temporally anticorrelated and hence not independent, so that their statistics become sub-Poissonian.

Let us consider if this self-regulation mechanism can account *quantitatively* for our measurements. For the sake of simplicity, we do not distinguish the two group V species. At temperature T, the nucleation probability P is dominated by factor $\exp[-\Delta G/(k_B T)]$, with $\Delta G = A/\Delta\mu$ the nucleation barrier and k_B Boltzmann's constant. Here, $\Delta\mu(c_{\mathrm{III}}, c_{\mathrm{V}}, T)$ is the difference of chemical potential per III–V pair between liquid with atomic concentrations c_i (i = III, V) and solid, and $A = \chi\omega h\gamma^2$, with ω the volume of a pair, h the height of a ML, γ the effective specific energy of the nucleus edge [4,20] and χ a geometric constant of the order of π. To first order,

$$\Delta\mu = \overline{\Delta\mu} + \alpha_{\mathrm{III}}\frac{\delta c_{\mathrm{III}}}{\bar{c}_{\mathrm{III}}} + \alpha_{\mathrm{V}}\frac{\delta c_{\mathrm{V}}}{\bar{c}_{\mathrm{V}}}, \qquad (1)$$

where overbars indicate some average reference state, $\alpha_i = \bar{c}_i(\partial\Delta\mu/\partial c_i)$ and $\delta c_i = c_i - \bar{c}_i$ [24]. Hence

$$P \approx \bar{P}\exp\left[\frac{A}{\overline{\Delta\mu}^2}\left(\frac{\alpha_{\mathrm{III}}}{k_B T}\frac{\delta c_{\mathrm{III}}}{\bar{c}_{\mathrm{III}}} + \frac{\alpha_{\mathrm{V}}}{k_B T}\frac{\delta c_{\mathrm{V}}}{\bar{c}_{\mathrm{V}}}\right)\right]. \qquad (2)$$

Let δN_i be the difference in numbers of group i atoms between current and reference liquid states, and $\bar{N}$ the total number of atoms in the latter. When one ML forms in a NW of radius R, then $\delta N_{\mathrm{III}} = \delta N_{\mathrm{V}} = -\pi R^2 h/\omega$. Assume that after the formation of a ML, the nanodrop refills with both constituents at the same rate. Then, at any time, $\delta N_{\mathrm{III}} = \delta N_{\mathrm{V}} = \delta N$. At typical NW radius, $\delta N/\bar{N} \ll 1$, so that $\delta c_i \approx (1 - 2\bar{c}_i)\delta N/\bar{N}$ and

$$P \approx \bar{P}\exp\left[\left(B_{\mathrm{III}}\frac{1-2\bar{c}_{\mathrm{III}}}{\bar{c}_{\mathrm{III}}} + B_{\mathrm{V}}\frac{1-2\bar{c}_{\mathrm{V}}}{\bar{c}_{\mathrm{V}}}\right)\frac{\delta N}{\bar{N}}\right], \qquad (3)$$

where dimensionless factors $B_i = \chi\omega h\gamma^2\alpha_i/(k_B T\overline{\Delta\mu}^2)$ contain parameters which are not precisely known but can be estimated. According to our thermodynamic calculations (to be presented elsewhere), α_{III} and α_{V} are of the same order (one to a few $k_B T$). Thus, B_{III} and B_{V} are also close to each other. Since $\bar{c}_{\mathrm{III}} \approx 0.5$, whereas $\bar{c}_{\mathrm{V}} \ll 1$, due to the low solubility of group V elements in the catalyst [9,16,17], the term $B_i\frac{1-2\bar{c}_i}{\bar{c}_i}$ is much larger for group V than for group III elements. Therefore, the group V atoms influence the probability of nucleation much more than the group III atoms. Moreover, the thinner the NW, the larger the effect, since $\delta N/\bar{N}$ scales as R^{-1}.

We simulated growth self-consistently from Eq. (3), considering only the effect of the variations of c_{V} on the nucleation probability [25]. Mean concentration $\bar{c}_{\mathrm{V}}$ was taken in the range of a few percent. As a first approximation, we assumed a constant refilling rate matching the average growth rate. The simulated nucleation events are markedly anticorrelated in time. The distributions of oscillation lengths and their standard deviations are consistent with the experimental ones [Fig. 2(b), Table I], which can for instance be reproduced with $B_{\mathrm{V}} = 2.5$ for $\bar{c}_{\mathrm{V}} = 0.02$ or $B_{\mathrm{V}} = 3.8$ for $\bar{c}_{\mathrm{V}} = 0.03$. Such B_{V} values are reasonable: for example, $B_{\mathrm{V}} = 3.8$ may be realized with plausible values of γ (0.4 J · m^{-2}), $\overline{\Delta\mu}$ (0.44 eV), and α_{V} ($2k_B T$).

Hence, the sub-Poissonian character of the nucleation statistics is perfectly explained by the negative feedback of the variation of the group V concentration in the liquid on the nucleation rate. Different drop refilling scenarios would lead to different quantitative estimates but would not alter this conclusion, provided the refilling of the drop is slower than its depletion upon the growth of one ML.

This self-regulation mechanism is remarkably efficient against length fluctuations in long NWs. To find out how the standard deviation varies for longer time periods (or higher average numbers $\bar{m}$ of nucleations per period), we count the nucleation events within sets of 1 to 6 consecutive oscillations. The deviation $\sigma^\star$ is calculated with respect to the average number of nucleation events in each multiple time period given by a linear fit to the full data set. Again, the prediction of our model agrees with the experiments: self-regulated growth quickly tends toward a $\bar{m}$-independent value of $\sigma^\star$, whereas Poisson nucleation would lead to $\sigma^\star = \sqrt{\bar{m}}$ (Fig. 3).

In conclusion, much information on NW growth can be gained from the method presented here. The method is rich

TABLE I. Data from 3 distinct NW segments of radius R, containing S oscillations. $\bar{m}$ is the mean number of MLs per oscillation and σ the measured standard deviation. σ_i and $\bar{m}^{1/2}$ are the inhomogeneous and homogeneous Poissonian standard deviations. Cumulated data are given for segments 2 and 3, which have similar R and $\bar{m}$.

Segment	R (nm)	S	$\bar{m}$	σ	σ_i	$\bar{m}^{1/2}$
1	24.8	17	24.81	2.26	5.10	4.98
2	25.3	17	18.03	1.98	4.44	4.25
3	24.7	21	18.99	1.49	4.46	4.36
2 and 3	(25)	38	18.57	1.75	4.39	4.31

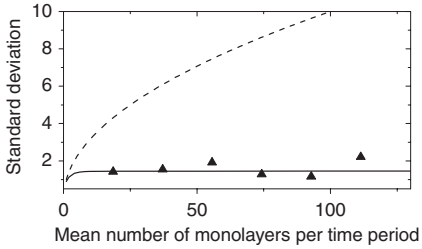

FIG. 3. Standard deviation of the number of MLs per time period when this period is varied. Triangles: experimental deviations $\sigma^{\star}$ obtained by counting the number of nucleation events within sets of 1 to 6 consecutive oscillations. Simulations for Poissonian statistics (dashed line) and self-regulated statistics (solid line) of nucleation events.

in potential extensions and not limited to VLS growth. Since weak composition modulations are detectable in HAADF mode, the requirement of having an alloy does not preclude the study of nearly pure-element NWs (e.g., Si with a low Ge content).

Our main result is the demonstration of a self-regulated growth mechanism that manifests itself by an antibunching of the nucleation events. This is very beneficial to the control of NW length: ensembles of NWs grown from catalyst particles of equal size should present very small fluctuations in length. However, the mechanism operates only if one NW constituent has a low solubility in the catalyst. The case of Au-catalyzed Si NWs, where the single constituent is highly soluble in the catalyst, is likely to be much less favorable in this respect. We thus confirm that the concentration of group V species in the catalyst is low, which explains why sharp interfaces are easier to obtain by swapping anions rather than cations.

The self-regulation mechanism stems from the impact of the rapid formation of a single ML on the chemical potential of the NW constituents in the catalyst. It is thus clearly specific to nucleation in nanovolumes, where the number of atoms consumed in the formation of a unit of the new phase (here a ML) following each nucleation is of the same order as the total number of these atoms in the parent phase. Also of import is that the nanovolume is an open system, where repeated nucleation is compensated by external fluxes. The sub-Poissonian character of the nucleation statistics manifests *temporal* anticorrelations between successive events. All of these features set the present effect apart from others, such as *spatially* non-Poissonian nucleation statistics (e.g., the depletion around a nucleus in a macroscopic supersaturated medium that precludes the formation of other nuclei in its vicinity [26]) or the decrease of nucleation probability induced in a closed system by the decrease of supersaturation. The extent to which the present effect affects the crystal structure of the NWs remains to be investigated.

This work was partly realized within Agence Nationale de la Recherche project BONAFO ANR-08-NANO-031.

*frank.glas@lpn.cnrs.fr

[1] P. Buffat and J. P. Borel, Phys. Rev. A **13**, 2287 (1976).
[2] E. Sutter and P. Sutter, Nano Lett. **8**, 411 (2008).
[3] E. Mendez-Villuendas and R. K. Bowles, Phys. Rev. Lett. **98**, 185503 (2007).
[4] F. Glas, J. C. Harmand, and G. Patriarche, Phys. Rev. Lett. **99**, 146101 (2007).
[5] R. S. Wagner and W. C. Ellis, Appl. Phys. Lett. **4**, 89 (1964).
[6] E. I. Givargizov, J. Cryst. Growth **31**, 20 (1975).
[7] V. G. Dubrovskii, N. V. Sibirev, J. C. Harmand, and F. Glas, Phys. Rev. B **78**, 235301 (2008).
[8] C.-Y. Wen, M. C. Reuter, J. Bruley, J. Tersoff, S. Kodambaka, E. A. Stach, and F. M. Ross, Science **326**, 1247 (2009).
[9] M. Tchernycheva, L. Travers, G. Patriarche, F. Glas, J.-C. Harmand, G. E. Cirlin, and V. G. Dubrovskii, J. Appl. Phys. **102**, 094313 (2007).
[10] M. C. Plante and R. R. LaPierre, J. Appl. Phys. **105**, 114304 (2009).
[11] S. A. Dayeh, E. T. Yu, and D. D. Wang, Nano Lett. **9**, 1967 (2009).
[12] V. G. Dubrovskii, N. V. Sibirev, G. E. Cirlin, A. D. Bouravleuv, Y. B. Samsonenko, D. L. Dheeraj, H. L. Zhou, C. Sartel, J. C. Harmand, G. Patriarche, and F. Glas, Phys. Rev. B **80**, 205305 (2009).
[13] D. L. Dheeraj, G. Patriarche, H. Zhou, J. C. Harmand, H. Weman, and B. Fimland, J. Cryst. Growth **311**, 1847 (2009).
[14] Y. Wu and P. Yang, J. Am. Chem. Soc. **123**, 3165 (2001).
[15] F. M. Ross, J. Tersoff, and M. C. Reuter, Phys. Rev. Lett. **95**, 146104 (2005).
[16] T. M. Massalski, *Binary Alloy Phase Diagrams* (American Society for Metals, Metals Park, OH, 1986), Vol. 1.
[17] C. Chatillon, F. Hodaj, and A. Pisch, J. Cryst. Growth **311**, 3598 (2009).
[18] E. Carlino and V. Grillo, Phys. Rev. B **71**, 235303 (2005).
[19] D. Kashchiev, Cryst. Growth Des. **6**, 1154 (2006).
[20] J. Johansson, L. S. Karlsson, C. P. T. Svensson, T. Mårtensson, B. A. Wacaser, K. Deppert, L. Samuelson, and W. Seifert, Nature Mater. **5**, 574 (2006).
[21] J. Johansson, L. S. Karlsson, K. A. Dick, J. Bolinsson, B. A. Wacaser, K. Deppert, and L. Samuelson, Cryst. Growth Des. **9**, 766 (2009).
[22] Since the average growth rate increases with time, the appropriate Poisson process is inhomogeneous. However, for the relatively short growth sequences studied here, the differences between homogeneous (constant growth rate) and inhomogeneous Poisson processes are very small and the distributions barely discernible. Accordingly, the two Poissonian standard deviations are very close (Table I).
[23] E. J. Schwalbach and P. W. Voorhees, Nano Lett. **8**, 3739 (2008).
[24] We neglect the small changes in Gibbs-Thomson effect due to possible changes of droplet volume [7].
[25] Including the variations of c_{III} has very little effect.
[26] R. A. Shaw, A. B. Kostinski, and M. L. Larsen, Q. J. R. Meteorol. Soc. **128**, 1043 (2002).